Crystal structure of the apoptotic suppressor CrmA in its cleaved form

Martin Renatus[1], Qiao Zhou[1,2], Henning R Stennicke[1], Scott J Snipas[1], Dušan Turk[3], Laurie A Bankston[4], Robert C Liddington[4] and Guy S Salvesen[1]*

Background: Cowpox virus expresses the serpin CrmA (cytokine response modifier A) in order to avoid inflammatory and apoptotic responses of infected host cells. The targets of CrmA are members of the caspase family of proteases that either initiate the extrinsic pathway of apoptosis (caspases 8 and 10) or trigger activation of the pro-inflammatory cytokines interleukin-1β and interleukin-18 (caspase 1).

Results: We have determined the structure of a cleaved form of CrmA to 2.26 Å resolution. CrmA has the typical fold of a cleaved serpin, even though it lacks the N-terminal half of the A helix, the entire D helix, and a portion of the E helix that are present in all other known serpins. The reactive-site loop of CrmA was mutated to contain the optimal substrate recognition sequence for caspase 3; however, the mutation only marginally increased the ability of CrmA to inhibit caspase 3. Superposition of the reactive-site loop of α1-proteinase inhibitor on the cleaved CrmA structure provides a model for virgin CrmA that can be docked to caspase 1, but not to caspase 3.

Conclusions: CrmA exemplifies viral economy, selective pressure having resulted in a 'minimal' serpin that lacks the regions not needed for structural integrity or inhibitory activity. The docking model provides an explanation for the selectivity of CrmA. Our demonstration that engineering optimal substrate recognition sequences into the CrmA reactive-site loop fails to generate a good caspase 3 inhibitor is consistent with the docking model.

Addresses: [1]Program in Apoptosis and Cell Death Research, The Burnham Institute, 10901 North Torrey Pines Road, La Jolla, CA 92037, USA, [2]Center for Blood Research, Harvard Medical School 800, Huntington Avenue Boston, MA 02115, USA, [3]Department of Biochemistry and Molecular Biology, Jo ef Stefan Institute, Ljubljana, Slovenia and [4]Program in Cell Adhesion, Extracellular Matrix Biology, The Burnham Institute, 10901 North Torrey Pines Road, La Jolla, CA 92037, USA.

*Corresponding author.
E-mail: gsalvesen@burnham.org

Key words: apoptosis, caspase, protease, protease inhibitor, serpin, viral countermeasures

Received: **3 April 2000**
Revisions requested: **4 May 2000**
Revisions received: **18 May 2000**
Accepted: **22 May 2000**

Published: **28 June 2000**

Structure 2000, **8**:789–797

0969-2126/00/$ – see front matter

Introduction

Animal development and homeostasis both depend on the ability of cells to die in an orderly fashion, by a process known as apoptosis. Apoptosis requires the participation of several members of a protease family known as the caspases [1,2]. Because animals remove viruses by inducing apoptosis in infected cells, viruses have evolved countermeasures that attempt to defeat the host's apoptotic response. One of the best known countermeasures is the caspase inhibitor known as cytokine response modifier A (CrmA) [3]. CrmA targets the apical caspase of the extrinsic apoptotic pathway (caspase 8), protecting the virus against apoptosis triggered by death receptor engagement [4,5]. CrmA also targets the pro-inflammatory cytokine activator (caspase 1), helping to prevent inflammatory signal transmission from infected cells [6,7]. The benefit to cowpoxvirus afforded by CrmA is substantial, as viruses devoid of the gene are drastically attenuated in infectivity and virulence [3,8].

On the basis of sequence conservation CrmA is classified as a member of the serpin family, which contains several protease inhibitors that target essential coagulation and fibrinolytic serine proteases [9]. CrmA differs from other serpins in that it is able to efficiently inhibit both cysteine proteases (caspases) and serine proteases (granzyme B and *Streptomyces griseus* protease E) that accept aspartate sidechains in their S1 pockets [10,11]. CrmA is thus a cross-class inhibitor, and illustrates the adaptability of serpins in their inhibition of proteases that utilize serine and cysteine catalytic nucleophiles; this property is not found in other active-site-directed protease inhibitor families [12].

In addition to its cross-class inhibitory property, CrmA is also a 'minimal' serpin. An alignment of CrmA with all other known serpins shows that it apparently lacks half of the A helix and the entire D helix, both of which are otherwise highly conserved throughout the serpin family and contain important regulatory sites. As discussed elsewhere [13], the serpin architecture seems to tolerate only a limited range of changes, so that serpins evolve against a strong selective pressure. As the serpin fold has been described by various authors [14], we will focus here primarily on the description of structural differences between CrmA and other serpins, and attempt to understand the inhibitory specificity of CrmA for individual caspases.

Figure 1

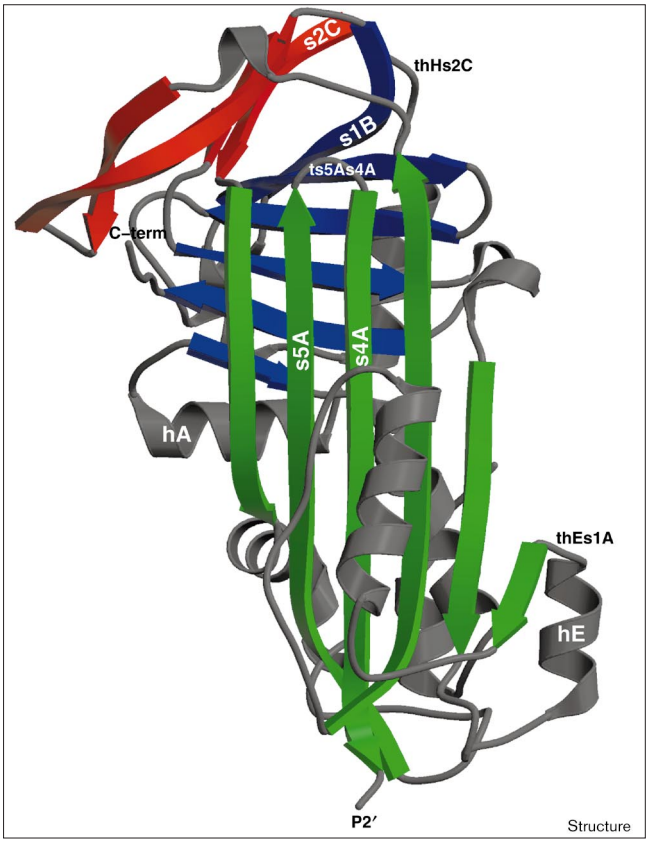

Ribbon diagram of cleaved CrmA. Secondary structure elements that are referred to in the text are named according to the nomenclature of Huber and Carrel [14]. The central β sheet A is colored in green, sheet B in blue, and sheet C in red. The figure was generated using the programs MOLSCRIPT [46] and Raster3D [47].

Table 1

Crystallographic data and refinement.

Data set		
Space group	$C222_1$	$P2_12_12_1$
Temperature (K)	298	100
Cell constants (Å)		
a,b,c	87.3, 136.3, 87.0	49.2, 92.5, 100.5
No. measurements	17,913	22,001
Completeness (%)		
overall/outermost shell	96.8/86.9*	98.7/94.5†
R_{merge}(%)		
overall/outermost shell	5.2/33.6*	5.0/28.6†
Number of atoms/asymmetric unit		
nonhydrogen protein atoms	2607	2607
solvent molecules	0	168 including 1DTT‡
Resolution range (Å)	50–2.5	50–2.26
No. reflections		
in refinement	17,693	21,293
to calculate R_{free}	1746	2100
Completeness (2σ cutoff) (%)	96.6	96.2
R/R_{free} (%)	30.7/35.3	22.77/27.2
Root mean square deviation		
bond lengths (Å)	0.009	0.015
bond angles (°)	1.36	1.72
mainchain/sidechain (Å)	1.18/1.56	1.31/1.66

*Outermost shell 2.53–2.49 Å; †outermost shell 2.33–2.26 Å. ‡The DTT molecule is in its reduced form; it interacts with Cys389.

Results and discussion

The CrmA structure

CrmA was expressed in *Escherichia coli*, purified, and treated with a catalytic amount of subtilisin Carlsberg, resulting in a cleavage of the peptide bond between Ala359 and Ser360 (sequence numbering throughout this paper is based on the topological similarity with α1-proteinase inhibitor). Cleaved CrmA crystallized in two different crystal forms (orthorhombic primitive, $P2_12_12_1$, and orthorhombic centered, $C222_1$). The structure was solved in both crystal forms and refined to an R factor of 23.2% (R_{free} of 27.7%) using the higher resolution data set (2.26 Å; $P2_12_12_1$). The structure of the lower resolution data set (2.5 Å; $C222_1$) could only be refined to an R factor of 29.8% (R_{free} of 35%) as the crystals turned out to have a significant level of merohedral twinning. A detailed summary of data collection and refinement statistics is given in Table 1.

The structure of CrmA shows the typical fold of a cleaved serpin (Figure 1), as first described for α1-proteinase inhibitor [15] and now observed in a variety of other structures including cleaved α1-antichymotrypsin [16], antithrombin [17,18], and leukocyte elastase inhibitor [19]. CrmA is an ellipsoidal molecule with dimensions 70 Å × 45 Å × 50 Å. Eighty percent of the amino acid residues are involved in three β sheets and eight α helices connected by mostly short loops and turns, forming a single large structural domain (Figure 1). In the final model most of the mainchain and sidechain atoms are defined by the electron density. Exceptions are the amino acids between residues 80 and 100 (see below) and some of the N-terminal and C-terminal residues. The structure from both crystal forms is virtually identical. The only differences are seen C-terminal to the cleavage site, from residue Ser360 to Asn363A (see below).

Despite its low sequence identity with other serpins, its unusual specificity and its ability to inhibit both serine and cysteine proteases, the overall structure of CrmA shows almost complete structural identity to serpins originating from other organisms. Optimal superposition of CrmA (341 residues) with human α1-antitrypsin (394 residues; Protein Data Bank [PDB] accession code 7API [15]) and horse leukocyte elastase inhibitor (379 residues; PDB code 1HLE [19]), using a distance cutoff of 1.5 Å, identifies 209 and 212 equivalent Cα positions, respectively; the respective root mean square deviations (rmsds) are 0.82 Å and 0.70 Å. The best fit obtained for the superimposition of CrmA with 7API and 1HLE is in the region of the three

Figure 2

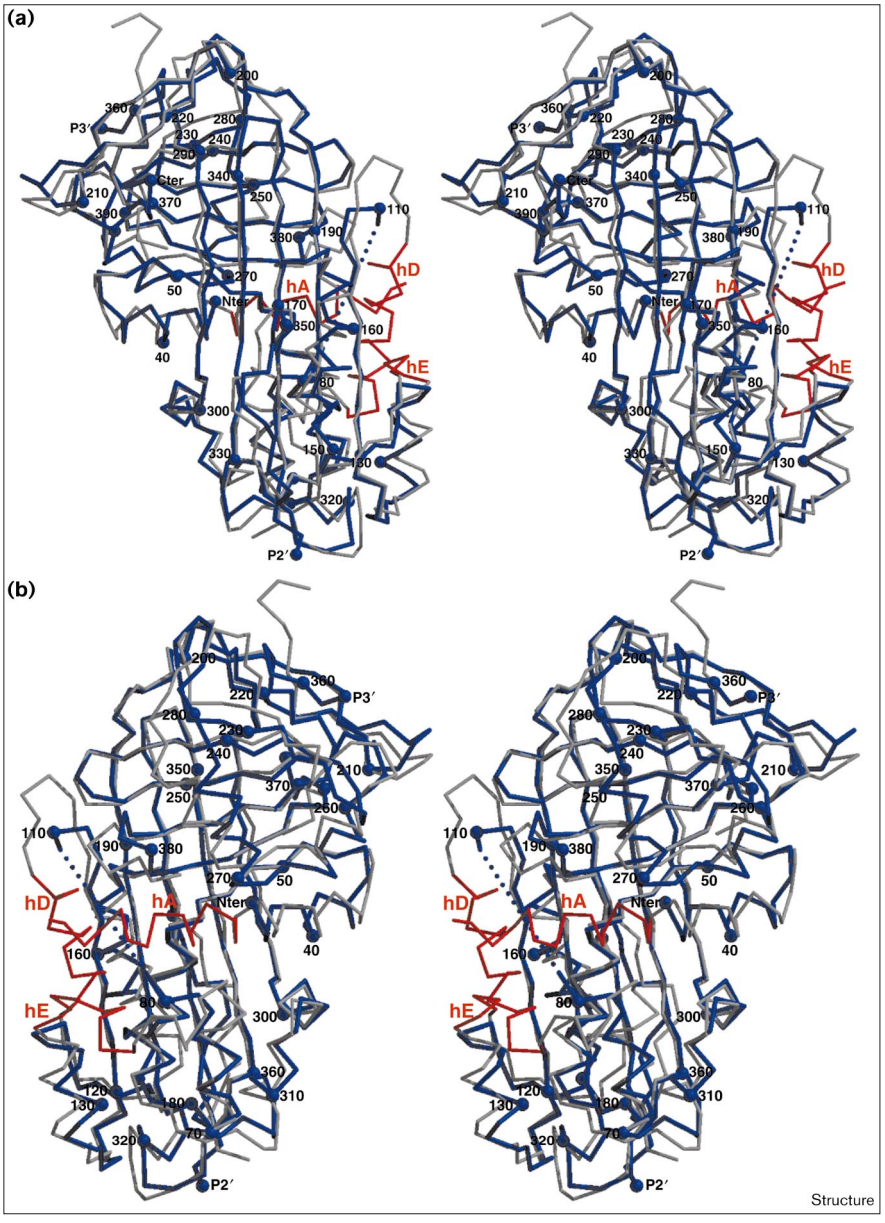

Superimposition of CrmA with human α1-proteinase inhibitor. CrmA is shown in blue and α1-proteinase inhibitor (PDB code 1PSI) is in gray. For clarity, the N-terminal residues Cys8 to Ser25 (numbering as in PDB file 1PSI, in α1-proteinase inhibitor residues −17 to −1) are not shown. Every tenth Cα atom in CrmA is highlighted. Three regions of the α1-proteinase inhibitor (half of the A helix, the entire D helix and parts of the E helix) are highlighted in orange. These regions are not present in CrmA and are the most prominent deletions in CrmA when compared with other members of the serpin family. The residues between Lys82 and Phe112 of CrmA are topologically equivalent to the D helix of α1-proteinase inhibitor. As these residues are undefined by electron density in the present structure, residues Lys82 and Phe112 are shown connected by a dotted line. **(a)** Stereoview Cα trace oriented as in Figure 1. **(b)** The molecule is rotated 180° around a vertical axis with respect to Figure 1. The figure was generated using the programs MOLSCRIPT [46] and Raster3D [47].

β sheets; the strongest deviations are seen in the helices on the back side of the molecule (Figure 2).

A structure-based sequence alignment of CrmA with human α1-proteinase inhibitor, human antithrombin, horse leukocyte elastase inhibitor and chicken ovalbumin shown in Figure 3. Residues are numbered on the basis of the superposition with α1-proteinase inhibitor, the archetype of the superfamily. This numbering system is used in all the paper.

CrmA as the minimal serpin

Compared with the α1-proteinase inhibitor and other known serpin structures, CrmA has three prominent deletions (Figures 2 and 3). These deletions are found on the 'east' side of the molecule (orientation as in Figure 1) and comprise the beginning of helix A, the entire helix D and the end of Helix E. Helix A is only half the normal length, and the distal end superim poses well with other known serpin structures. The N-terminal residue Met36 is not accessible to solvent. The sidechain of this residue is buried in a hydrophobic groove formed by the residues Leu267, Phe272, Val373, Ile382 and Val385. The electron density shows no indication of an N-terminal modifications; the N-terminal amino group forms a salt bridge to the sidechain of Asp269.

Figure 3

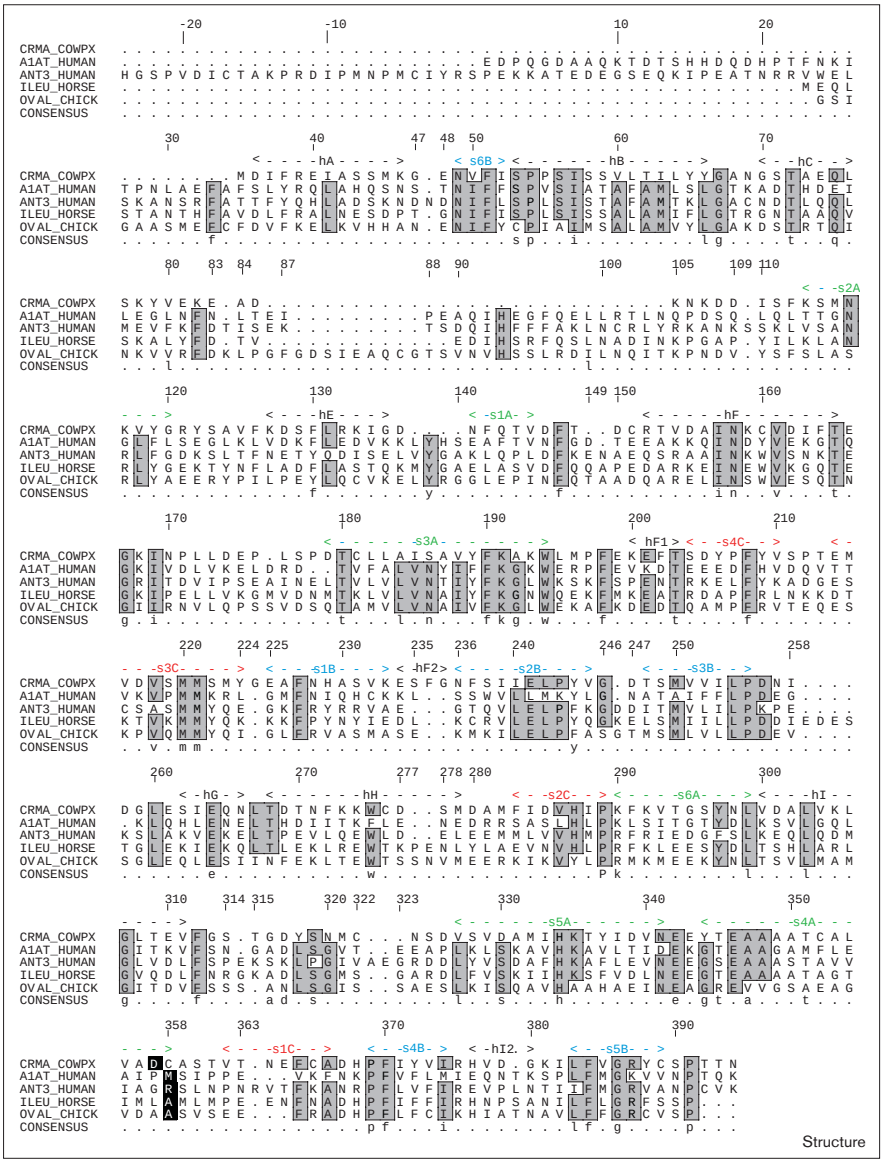

Structure-based sequence alignment. The alignment includes CrmA from cowpox (CRMA_COWPX) human α1-proteinase inhibitor (PDB code 7API; A1AT_HUMAN), human antithrombin (PDB code 7API ANT3_HUMAN), horse leukocyte elastase inhibitor (PDB code 1HLE; ILEU_HORSE) and chicken ovalbumin (PDB code 1OVA; OVAL_CHICK). The alignment was generated using the program ALSCRIPT [48]. Gray boxes identify residues identical in at least three of the five sequences. The black boxes identify the P1 residues; note that the P1 residue in CrmA is shifted by one residue relative to all other shown serpins. The consensus sequence is the Munich Information Centre for Protein Sequences serpin family (family 00998) consensus from the appropriate database (http://www.mips.biochem.mpg.de.) Secondary structure elements are colored as shown in Figure 1 and named following the nomenclature of Huber and Carell [14].

In both crystal forms no interpretable electron density could be found for residues Lys82 to Phe112, corresponding to 12 consecutive amino acids of the primary sequence (see Figure 3). Sodium dodecyl sulfate polyacrylamide gel electrophoresis (SDS–PAGE) analysis of the crystals shows no indication of any cleavage in this segment. Weak electron density for residues Glu83 to Asp85 shows no indication for a helical conformation, but instead suggests an extended conformation. The five residues from Lys105 to Asp109 show no electron density, and the gap is of a size consistent with a short loop.

Adjacent to the D loop of CrmA is a four amino acid deletion (residues 137–140 in α1-proteinase inhibitor) at the end of helix E and in turn hEs1A. Interestingly, this includes the deletion of a tyrosine residue that is highly conserved in the serpin family (Tyr138 in α1-proteinase inhibitor) [14]. In α1-proteinase inhibitor and horse leukocyte elastase inhibitor, Tyr138 Oε hydrogen bonds to His93 Nδ of helix D and clusters with Met63, Leu66 and Phe82, all residues that are highly conserved among the serpins but mutated in CrmA. The probable function of these interactions is to stabilize the conformation of helix D. With the deletion of helix D in CrmA the selective pressure to conserve the residues at positions 63, 66, 82 and the segment of residues 137–140 is lost.

The D helix is known to be a regulatory site in other serpins. For example, the D helix of antithrombin and heparin cofactor 2 contain heparin-binding elements that

Figure 4

Stereoview of the electron density. Parts of the central β sheet A (strands 3A, 4A, 5A and 6A, right to left, and turn s5As4A) are superimposed with the final $2F_o–F_c$ electron-density map contoured at 0.8σ. The atoms are colored by type: blue, carbon; cyan, nitrogen; and red, oxygen. The figure was made with the program BobScript [49].

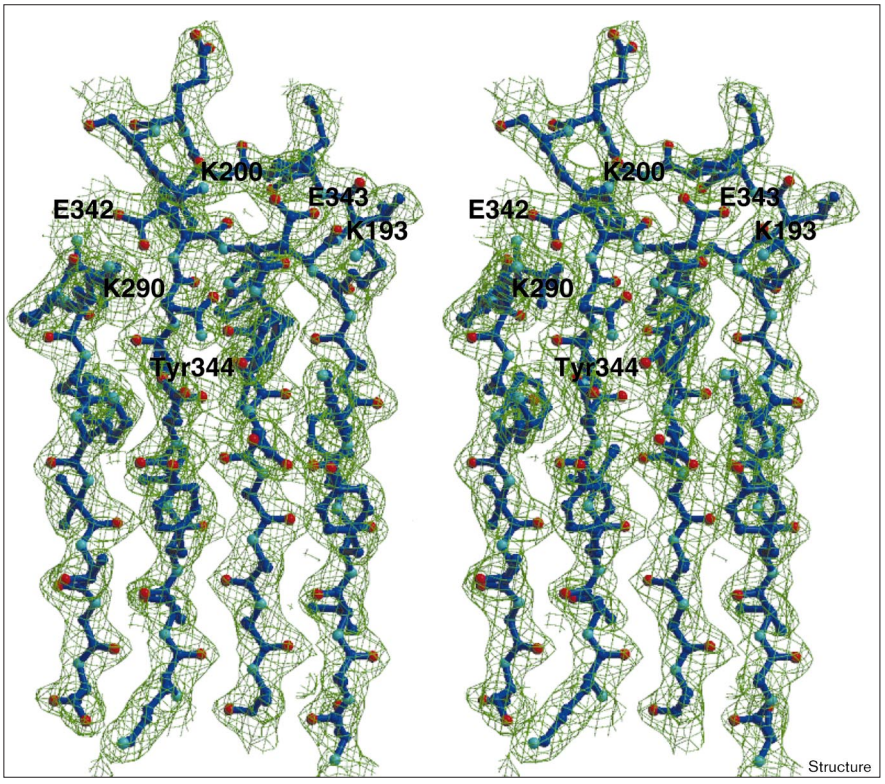

activate these serpins for inhibition of their target proteases [20,21]. Furthermore, the antiapoptotic function of plasminogen activator inhibitor 2 requires sequences adjacent to the D helix [22] and the nuclear translocation signal in bomabin is located in the D helix [23]. We conclude that this regulatory patch has been abolished in CrmA, and surmise that CrmA is not a cofactor-regulated serpin. Interestingly, the linker sequence that replaces the D helix is the most variable region in CrmA homologs from other pox viruses, such as vaccinia, smallpox and cowpox viruses, which are otherwise more than 90% identical.

The reactive-site loop

For this study the reactive-site loop (RSL) was cleaved with a catalytic amount of the protease subtilisin Carlsberg, between the residues Ala359 and Ser360 (P2′–P3′). This cleavage site is two residues upstream of the physiological cleavage site Asp357–Cys358 (P1–P1′). As seen in the structures of several other serpins, CrmA adopts the so-called 'relaxed' conformation with the two residues flanking the cleavage site separated by 70 Å. The upstream segment from residue Tyr344 to Ala359 (P15–P2′) becomes inserted into β sheet A forming its central strand s4A. This observation demonstrates that CrmA can utilize the classic RSL-insertion mechanism in spite of being a minimal serpin.

In contrast to the upstream segment of the RSL, the downstream segment, Ser360 to Asn363A (P3′–P7′), only makes a few interactions with the rest of the molecule and is therefore rather flexible. In the orthorhombic primitive ($P2_12_12_1$) crystal form this segment runs roughly antiparallel to strand s1B forming hydrogen bonds. The carbonyl oxygen atoms of Ser360 and Val362 are hydrogen bonded to Lys233 Nζ and Ser231 Oγ, respectively. In the twinned crystal form ($C222_1$) residues Ser360 to Glu363B are in an extended conformation. They contact residues 213–216 (strand s3C) of a symmetry-related molecule in a β-sheet-like interaction, yet there is no indication of oligomerization that is sometimes seen in RSL-cleaved serpins (see the crystal structures of α1-anti-trypsin with PDB codes 1QMB and 1D5S).

Unusual features of the RSL

The protease inhibitory mechanism of serpins is thought to require, at an early stage, the insertion into the central β sheet A of several residues in the segment surrounding residue 345 [24–27]. This segment, called the 'hinge region', appears to be unusual in CrmA. All known serpins (there are more than 100 sequences in the Protein families database of alignments and HMMS database; http://www.sanger.ac.uk/Pfam) contain a glycine at position 344, with just two exceptions — CrmA and the related orthopoxvirus serpin B24R (also known as Spi1).

Figure 5

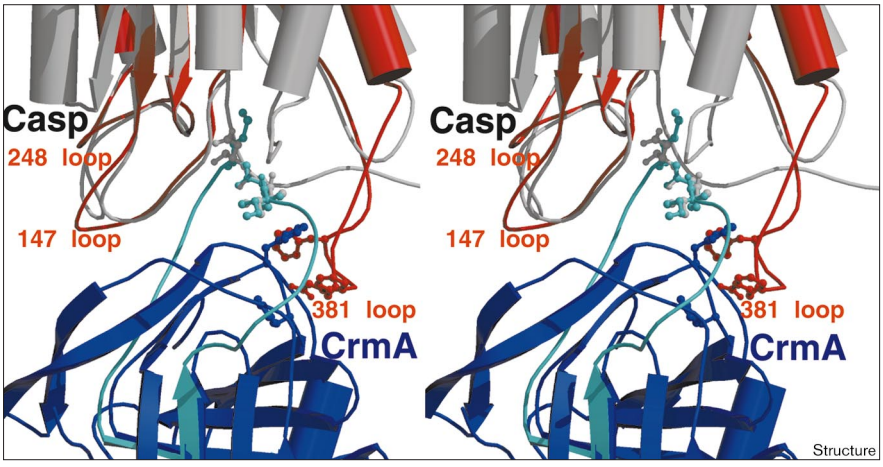

Stereoview docking model of CrmA with caspases 1 and 3. The upper molecules show the equivalent substrate-binding regions of caspase 1 in gray and caspase 3 in red. The intact reactive-site loop in cyan is modeled onto the CrmA structure in blue using the structure of active α1-proteinase inhibitor (1PSI). Surface loops of caspase 3 that differ from caspase 1 are highlighted in red. The most prominent difference between caspases 3 and 1 is the 381 loop, a ten-residue insertion compared to caspase 1 that defines the S4 subsite specificity of caspase 3. The sidechain residues of caspase 3 residues Phe381d, Asp381e and Phe381f are shown in ball-and-stick representation. There is no indication of any steric clashes between caspase 1 and CrmA. However, the 381 loop of caspase 3 would overlap with Phe227 at the end of s1B in the CrmA molecule, causing unfavorable interactions and explaining the weak inhibition of caspase 3 by CrmA.

Both serpins possess a tyrosine at this position, and in the structure of cleaved CrmA Tyr344 is the fourth residue in the α turn s5As4A. The sidechain of Tyr344 points from the molecular surface into the solvent without making any unusual contacts. This residue is well defined by electron density (see Figure 4), and the temperature factors do not suggest any higher mobility. The ϕ,ψ angles of Tyr344 lie in the allowed region of the Ramachandran plot.

Evidently, Tyr344 does not hamper the conformation of the cleaved CrmA. But might it influence the conformation of the RSL in the uncleaved (inhibitory) conformation? We modeled the substitution of tyrosine for the consensus Gly344 in the known structures of uncleaved, resting serpins. In all cases, this required only minor changes of some sidechain torsion angles. Consequently we assume that Tyr344 does not influence the resting, inhibitory conformation of CrmA and that this conformation would be similar to that of other serpins.

To test the importance of Tyr344 we cloned, expressed and purified a CrmA mutant with a glycine residue at this position (Tyr344→Gly). The rate of inhibition and stability of the resulting complex of caspase 8 with the mutant CrmA (k_{on} 3.6×10^5 M^{-1} s^{-1}) showed no difference to wild-type (k_{on} 3.5×10^5 M^{-1} s^{-1}), and there is no sign of an altered partition ratio for the mutant (data not shown). The partition ratio defines the number of inhibitor molecules needed for complete inhibition of the target protease, and is heavily influenced by mutations in the RSL of other serpins [28]. The only difference we could ascribe to the Tyr344Gly mutant was a slight but consistent increase in stability at elevated temperature ($t_{1/2}$, 46°C = 200 min) compared with wild-type CrmA ($t_{1/2}$, 46°C = 120 min). Therefore, on the basis of our *in vitro* observations, we conclude that Tyr344 would not influence the inhibitory mechanism of CrmA under normal conditions expected during viral infection *in vivo*.

Specificity for caspases

CrmA does not inhibit all caspases with the same efficiency. It is a strong inhibitor of caspases 1 and 8, but a much weaker inhibitor of caspase 3 [4]. In order to understand the selectivity of CrmA for caspase 1 over caspase 3 we constructed a mutant with an altered RSL sequence, the idea being to increase the selectivity of CrmA for caspase 3. Positional scanning to determine the P4–P2 subsite preferences of caspases [29] showed that the sequence Leu-Val-Ala (P4–P2 in wild-type CrmA) is not optimal for recognition by caspase 3. Therefore, we changed P4–P2 into Asp-Glu-Val, the preferred caspase 3 substrate sequence, on the grounds that presenting an optimal substrate sequence should provide increased inhibitory power. As expected, the inhibition rate against caspases 1 and 8 dropped dramatically (k_{on} decreased by two to three orders of magnitude). In addition, a moderate increase in caspase 3 inhibition was achieved (k_{on} increased from 1.6×10^2 M^{-1} s^{-1} for the wild type to 1.4×10^3 M^{-1} s^{-1} for the mutant). These results confirm the importance of the RSL sequence in determining the affinity of CrmA for caspases 1 and 8. However, the mutant is still a poor inhibitor of caspase 3, even though it now contains an optimal substrate-binding sequence. A similar failure to direct the specificity of CrmA towards caspase 3 based on comparable mutants has been identified previously [30]. Together, these results indicate that additional interactions distinct from those in the substrate cleft allow good inhibition of caspases 1 and 8, but prevent potent inhibition of caspase 3.

Madison and his colleagues [31] identified the signi ficance of secondary interaction sites, distant from the substratebinding cleft, in the inhibition of proteases by serpins. To identify additional interaction sites we generated a docking model between CrmA and caspases 1 and 3. The structure of CrmA described in this paper is that of a relaxed, non-inhibitory serpin, but several structures of uncleaved serpins are available. The RSL in these different structures adopts various conformations, suggesting that this region is highly flexible. There is an ongoing discussion about which structure is the closest model of the 'docking' conformation — the conformation adopted by serpins in the initial complex. It seems reasonable to assume, however, that the structure of intact α1-proteinase inhibitor (PDB code 1PSI) might show this docking conformation, as residues P3–P1 (Ile356, Pro357 and Met358) adopt a substrate-like conformation with Met358 pointing away from the molecular surface. We therefore modeled the RSL of intact α1-proteinase inhibitor onto the structure of cleavage CrmA and superimposed this model with caspase 1 (1ICE) or caspase 3 (1PAU). The putative RSL was superimposed with the tetrapeptide aldehyde inhibitor (Ac-Tyr-Val-Ala-Asp-CHO) bound to capase 1 or the equivalent Asp-Glu-Val-Asp inhibitor bound to caspase 3. The resulting models are shown in Figure 5. This modeling predicts no unfavorable interactions between caspase 1 and the putative docking form of CrmA. CrmA is also a good inhibitor of caspase 8 [4], and visual inspection of the caspase 8 structures [32,33] predicts no unfavorable interactions. On the other hand, docking to caspase 3 leads to severe clashes between the 381 loop of caspase 3 [34] and residues around Phe227 (strand s1B) and Phe283 (turn thHs2C) on the surface of CrmA. The caspase 3 coordinates do not indicate a high mobility of this loop, although the B factors in this exposed region are higher than in the core of the molecule. Therefore, in developing the 381 loop presumably as a requirement for substrate specificity, caspase-3 has also eliminated the possibility of physiological inhibition by CrmA. Interestingly, CrmA and the CrmA P4–P2 mutant are both extremely weak inhibitors of caspase 7, the other executioner caspase. Although the structure of caspase 7 has not been determined, it is predicted to share with caspase 3 a similar extended 381 loop and comparable extended substrate specificity. Consequently, inhibition of caspases 3 and 7 (the execution phase of apoptosis) by a serpin would require a much more extended RSL than is seen in any of the known structures. Interestingly, p35 the caspase inhibitor from baculovirus, although not a serpin, does have such an extended RSL [35] and inhibits caspases 1, 3 and 8 equally well [36].

Biological implications

Orthopox viruses, including smallpox and cowpox virus, are among the deadliest mammalian pathogens. Part of their virulence is due to the large number of proteins that are apparently used to defeat the host's response to viral infection; these proteins are encoded by the 'host-range' genes. The serpin CrmA is an important host-range gene product that is necessary for the survival of viral-infected cells, where it blocks the release of pro-inflammatory mediators and prevents apoptosis of infected cells. Significantly, CrmA does not block the execution phase of apoptosis that is mediated by caspases 3 and 7, but only blocks the initiation phase mediated by caspase 8 (and possibly caspase 10).

CrmA lacks regulatory regions found in other serpins and the conserved Gly344 residue is replaced by a tyrosine. Despite these changes, the structure of cleaved CrmA is nearly identical to that of other cleaved serpins. The fact that CrmA tolerates a tyrosine at position 344 suggests that the central β sheet A is more flexible than that found in other serpins and is readily able to accommodate the insertion of the bulkier tyrosine residue. One possibility is that the loss of the D helix in CrmA is responsible for this increase in flexibility, as this helix is positioned so as to hinder strand separation and is the principal site of regulation in other serpins.

Modeling the CrmA structure onto homologous serpins indicates that severe steric clashes with a loop on caspase 3 would prevent significant inhibition, and that it might not be possible to evolve an inhibitor of the executioner caspases based on the serpin frame. Indeed, it may not have been necessary for orthopox viruses to evolve an inhibitor of the execution phase, since blocking the initiation phase would be the most economic strategy.

Materials and methods

CrmA expression and purification

The expression in *E. coli* of a C-terminal His_6-tagged CrmA (Genbank accession number P07385) has been described elsewhere [10]. To obtain a CrmA construct lacking the His_6 tag, the coding sequence from the pFLAG-1 construct including a stop codon, was subcloned into pET21d (Novagen) using *Nco* I/*Xho* I cleavage sites. This construct was expressed in *E. coli* strain BL21(DE3)pLysS. Cells were collected after a 6 h induction at 30°C with 0.3 mM isopropyl-β-D-thiogalactopyranoside (IPTG), resuspended in 100 mM NaCl, 50 mM Tris pH 8, lysed by freeze/thaw and by sonication, and centrifuged. The lysate of a 1.5 l culture was diluted into 500 ml buffer containing 20 mM NaCl, 10 mM Tris, pH 8 and 1 mM dithiothreitol (DTT) and loaded on a 10 ml DEAE-Sepharose (Sigma) column. CrmA eluted between 200 and 300 mM NaCl, 20 mM Tris pH 8. These fractions were pooled, dialyzed against 20 mM NaCl, 10 mM Tris (pH8), 1 mM DTT and loaded onto a 1 ml Mono Q column (Pharmacia). CrmA eluted between 240 and 290 mM NaCl.

Virgin CrmA was cleaved at 37°C for 30 min by subtilisin Carlsberg (purchased from Sigma, P5380) in 100 mM NaCl, 50 mM Tris pH 8, 10 mM DTT, 1 mM $CaCl_2$ using a 200:1 molar ratio of CrmA:subtilisin. The reaction was stopped by adding phenylmethane sulphonyl fluoride (100 times molar excess based on subtilisin concentration). The reaction mixture was re-purified on a Mono Q column.

Protein crystallization and structure analysis

Crystals were grown using the sitting-drop vapor diffusion method at protein concentrations of 7–10 mg/ml at 4°C and 23°C. First crystals grew within two weeks at 4°C by mixing 1 µl protein with 0.7 µl reservoir solution (0.1 M Na acetate pH 5, 20% PEG 4000). Crystals of sufficient quality for X-ray diffraction experiments and structure refinement were obtained at two different conditions: 0.2–0.3 M Na phosphate, 20% PEG 4000 (4°C); and 0.1 M Na acetate pH 5–6, 15% PEG 4000, 0.1 M $MgCl_2$ (23°C). They grew between one week and several months and belonged to the space groups $C222_1$ and $P2_12_12_1$ (see Table 1). Data were collected on an R-AXIS IV image plate mounted on a Rigaku rotating anode ($C222_1$) and at the X-25 beamline in Brookhaven ($P2_12_12_1$). Data were processed and scaled in DENZO/SCALEPACK [37].

The data set from the $C222_1$ crystal form was the first available. The structure was solved using Patterson techniques with the program AMoRe [38] (integration radius 30 Å, resolution range 10–4 Å) and the structure of cleaved horse leukocyte elastase inhibitor (1HLE) as search model. Both rotational and translational searches gave clear peaks (12.5 sigma versus 6.6 and 27.0 sigma versus 23.7); after rigid-body refinement the correlation factor was 28.7%. Map interpretation has been done in MAIN [39], crystallographic refinement (simulated annealing, positional and temperature-factor refinement) in CNS [40] using the parameters of Engh and Huber [41]. Although almost all residues, except for residues of the D helix and some terminal residues, could be fitted into the electron density, the R factor did not drop below 30% (R_{free} 35.5%). Data analysis as described by Yeates [42] indicated merohedral twinning as a reason for the problems with data refinement. The degree of twinning was estimated to be between 20% to 30%. The twinning is a result of a 180° rotation along the diagonal of the *ac* plane. In the space group $C222_1$ this is only possible if the axis *a* and *c* are of equal length. However, crystallographic refinement in SHELX [43], a program that allows the refinement of the twining factor α as an independent parameter, did not improve the R factor or the electron density.

The structure was finished after the data set from $P2_12_12_1$ became available. An unfinished CrmA structure from the $C222_1$ data set was used to locate the molecule in the $P2_12_12_1$ packing. The Patterson search was done in AMoRe and gave a clear solution with a correlation factor of 58.9%. With this data the structure could be refined to an R factor of 23.3% (a summary of the refinement statistics is given in Table 1). In the final model 329 out of 341 residues are defined by electron density.

Inhibition kinetics

Recombinant caspases were purified and characterized as previously described [44], and inhibition by CrmA and CrmA mutants was followed by the method of progress curves in reactions containing at least a tenfold molar excess of inhibitor [4], using carbobenzoxy-Asp-Glu-Val-Asp-7-amino-4-trifluoromethyl coumarin as reporter substrate. Apparent inhibition rate constants were determined during the approach to steady state of substrate hydrolysis, and were determined by the method of progress curves, where a reaction was initiated by the addition of enzyme to a mixture of substrate and inhibitor. The inhibitor concentration was kept at a large excess of enzyme to render the reaction pseudo-first order for convenience of analysis. Calculations of kinetic parameters are based on a single-step reaction scheme [4].

The first order rate constant (k_{obs}) was derived from:

$$\ln([P]_{t+\Delta t} - [P]_t) = C - k_{obs}t \quad (1)$$

where $[P]_{t+\Delta t}$ is the product concentration at time $t+\Delta t$ of the association reaction and $[P]_t$ is the product concentration at time t [45]. The second order rate constant (k_a) was derived according to the following relationship:

$$k_a = (k_{obs}/I)(1 = S/K_m) \quad (2)$$

where S is the concentration of substrate and K_m is the Michaelis constant.

Accession numbers

The coordinates of CrmA in its cleaved form have been deposited in the Protein Data Bank with accession code 1F0C.

Acknowledgements

We thank Annamarie Price for help with expressing proteins, José de Pereda, Chao-Zhou Ni and Karl-Peter Hopfner for their input in data processing and structure refinement, and Ed Madison for comments on the manuscript. This work was supported by National Institutes of Health grant HL51399 to GSS, and a fellowship from the Deutschen Akademischen Austauschdienst to MR.

References

1. Salvesen, G.S. & Dixit, V.M. (1997). Caspases: intracellular signaling by proteolysis. *Cell* **91**, 443-446.
2. Thornberry, N.A. & Lazebnik, Y. (1998). Caspases: enemies within. *Science* **281**, 1312-1306.
3. Ray, C.A., *et al*., & Pickup, D.J. (1992). Viral inhibition of inflammation: cowpox virus encodes an inhibitor of the interleukin-1β-converting enzyme. *Cell* **69**, 597-604.
4. Zhou, Q., Snipas, S., Orth, K., Dixit, V.M. & Salvesen, G.S. (1997). Target protease specififity of the viral serpin CrmA: analysis of five caspases. *J. Biol. Chem.* **273**, 7797-7800.
5. Walsh, C.M., Wen, B.G., Chinnaiyan, A.M., O'Rourke, K., Dixit, V.M. & Hedrick, S.M. (1998). A role for FADD in T cell activation and development. *Immunity* **8**, 439-449.
6. Komiyama, T., *et al*., & Salvesen, G. (1994). Inhibition of interleukin-1beta converting enzyme by the cowpox virus serpin CrmA. An example of cross-class inhibition. *J. Biol. Chem.* **269**, 19331-19337.
7. Turner, S., Kenshole, B. & Ruby, J. (1999). Viral modulation of the host response via crmA/SPI-2 expression. *Immunol. Cell Biol.* **77**, 236-241.
8. Pickup, D.J., Ink, B.S., Hu, W., Ray, C.A. & Joklik, W.K. (1986). Hemorrhage in lesions caused by cowpox virus is induced by a viral protein that is related to plasma protein inhibitors of serine proteases. *Proc. Natl Acad. Sci. USA* **83**, 7698-7702.
9. Potempa, J., Korzus, E. & Travis, J. (1994). The serpin superfamily of proteinase inhibitors: structure, function, and regulation. *J. Biol. Chem.* **269**, 15957-15960.
10. Quan, L.T., Caputo, A., Bleackley, R.C., Pickup, D.J. & Salvesen, G.S. (1995). Granzyme B is inhibited by the cowpox virus serpin CrmA. *J. Biol. Chem.* **270**, 10377-10379.
11. Komiyama, T., Quan, L.T. & Salvesen, G.S. (1996). Inhibition of cysteine and serine proteinases by the cowpox virus serpin CrmA. *Adv. Exp. Med. Biol.* **389**, 173-176.
12. Bode, W. & Huber, R. (1992). Natural protein proteinase inhibitors and their interaction with proteinases. *Eur. J. Biochem.* **204**, 433-451.
13. Marshall, C.J. (1993). Evolutionary relationships among the serpins. *Phil. Trans. R. Soc. Lond. B* **342**, 101-119.
14. Huber, R. & Carrell, R.W. (1989). Implications of the three-dimensional structure of α_1-antitrypsin for structure and function of serpins. *Biochemistry* **28**, 8966-8971.
15. Loebermann, H., Tokuoka, R., Deisenhofer, J. & Huber, R. (1984). Human α_1-proteinase inhibitor: crystal structure analysis of two modifications, molecular model and preliminary analysis of the implications for function. *J. Mol. Biol.* **177**, 531-556.
16. Baumann, U., Huber, R., Bode, W., Grosse, D., Lesjak, M. & Laurell, C.B. (1991). Crystal structure of cleaved human α_1-antichymotrypsin at 2.7 Å resolution and its comparison with other serpins. *J. Mol. Biol.* **218**, 595-606.
17. Schreuder, H., *et al*., & Theunissen, H. (1993). Crystallization and preliminary X-ray analysis of human antithrombin III. *J. Mol. Biol.* **229**, 249-250.
18. Mourey, L., Samama, J.P., Delarue, M., Petitou, M., Choay, J. & Moras, D. (1993). Crystal structure of cleaved bovine antithrombin III at 3.2 Å resolution. *J. Mol. Biol.* **232**, 223-241.
19. Baumann, U., Bode, W., Huber, R., Travis, J. & Potempa, J. (1992). Crystal structure of cleaved equine leucocyte elastase inhibitor determined at 1.95 Å resolution. *J. Mol. Biol.* **226**, 1207-1218.
20. Carrell, R.W., Stein, P.E., Fermi, G. & Wardell, M.R. (1994). Biological implications of 3 Å structure of dimeric antithrombin. *Structure* **2**, 257-270.

21. Whinna, H.C., Blinder, M.A., Szewczyk, M., Tollefsen, D.M. & Church, F.C. (1991). Role of lysine 173 in heparin binding to heparin cofactor II. *J. Biol. Chem.* **266**, 8129-8135.
22. Dickinson, J.L., Norris, B.J., Jensen, P.H. & Antalis, T.M. (1998). The C-D interhelical domain of the serpin plasminogen activator inhibitor-type 2 is required for protection from TNF-alpha induced apoptosis. *Cell Death Differ.* **5**, 163-171.
23. Chuang, T.L. & Schleef, R.R. (1999). Identification of a nuclear targeting domain in the insertion between helices C and D in protease inhibitor-10. *J. Biol. Chem.* **274**, 11194-11198.
24. Gettins, P., Patston, P.A. & Schapira, M. (1993). The role of conformational changes in serpin structure and function. *BioEssays* **15**, 461-467.
25. Wright, H.T. & Scarsdale, J.N. (1995). Structural basis for serpin inhibitor activity. *Proteins* **22**, 210-225.
26. Elliott, P.R., Lomas, D.A., Carrell, R.W. & Abrahams, J.P. (1996). Inhibitory conformation of the reactive loop of alpha 1-antitrypsin. *Nat. Struct. Biol.* **3**, 676-681.
27. Schulze, A.J., Frohnert, P.W., Engh, R.A. & Huber, R. (1992). Evidence for the extent of insertion of the active site loop of intact α1-proteinase inhibitor in β-sheet A. *Biochemistry* **31**, 7560-7565.
28. Hood, D.B., Huntington, J.A. & Gettins, P.G.W. (1994). α_1-Proteinase inhibitor variant T345R. Influence of P14 residue on substrate and inhibitory pathways. *Biochemistry* **33**, 8538-8547.
29. Thornberry, N.A., *et al.*, & Nicholson, D.W. (1997). A combinatorial approach defines specificities of members of the caspase family and granzyme B. *J. Biol. Chem.* **272**, 17907-17911.
30. Ekert, P.G., Silke, J. & Vaux, D.L. (1999). Inhibition of apoptosis and clonogenic survival of cells expressing crmA variants: optimal caspase substrates are not necessarily optimal inhibitors. *EMBO J.* **18**, 330-338.
31. Madison, E.L., Goldsmith, E.J., Gerard, R.D., Gething, M.J. & Sambrook, J.F. (1989). Serpin-resistant mutants of human tissue-type plasminogen activator. *Nature* **339**, 721-724.
32. Blanchard H., *et al.*, & Grutter M.G. (1999). The three-dimensional structure of caspase-8: an initiator enzyme in apoptosis. *Structure* **7**, 1125-1133.
33. Watt W., Koeplinger K.A., Mildner A.M., Heinrikson R.L., Tomasselli A.G. & Watenpaugh K.D. (1999). The atomic-resolution structure of human caspase-8, a key activator of apoptosis. *Structure* **7**, 1135-1143.
34. Rotonda, J., *et al.*, & Becher, J.W. (1996). The three-dimensional structure of apopain/CPP32, a key mediator of apoptosis. *Nat. Struct. Biol.* **3**, 619-625.
35. Fisher, A.J., Cruz, W., Zoog, S.J., Schneider, C.L. & Friesen, P.D. (1999). Crystal structure of baculovirus P35: role of a novel reactive-site loop in apoptotic caspase inhibition. *EMBO J.* **18**, 2031-2039.
36. Zhou, Q., *et al.*, & Salvesen, G.S. (1998). Interaction of the baculovirus anti-apoptotic protein p35 with caspases: specificity, kinetics, and characterization of the caspase/p35 complex. *Biochemistry* **37**, 10757-10765.
37. Otwinowski, Z. & Minor, W. (1997). Processing of X-ray diffraction data collected in oscillation mode. *Methods Enzymol.* **276**, 307-326.
38. Navazza, J. (1994). AMoRe: an automated package for molecular replacement. *Acta Crystallogr. A* **50**, 157-163.
39. Turk D. (1992). *Weiterentwicklung eines Programmes für Molekülgraphik und Elektronendichte-Manipulation und seine Anwendung auf verschiedene Protein-Strukturaufklärungen.* PhD Thesis, Technische Universität, München, Germany.
40. Brünger, A.T., *et al.*, & Warren, G.L. (1998). Crystallography & NMR system (CNS): a new software suite for macromolecular structure determination. *Acta Crystallogr. D* **54**, 905-921.
41. Engh, R.A. & Huber, R. (1991). Accurate bond and angle parameters for X-ray protein-structure refinement. *Acta Crystallogr. A* **47**, 392-400.
42. Yeates, T.O. (1997). Detecting and overcoming crystal twinning. *Methods Enzymol.* **276**, 344-358.
43. Sheldrick, G.M. & Schneider, T.R. (1997). SHELXL: high resolution refinement. *Methods Enzymol.* **277**, 319-343.
44. Stennicke, H.R. & Salvesen, G.S. (1999). Caspases: preparation and characterization. *Methods* **17**, 313-319.
45. Knight, C.G. (1986). The characterization of enzyme inhibition. In *Proteinase Inhibitors.* (Barrett, A.J. & Salvesen, G. eds) pp. 23-51, Elsevier Science Publishers BV, Amsterdam.
46. Kraulis, P. J. (1991). MOLSCRIPT: a program to produce both detailed and schematic plots of protein structures. *J. Appl. Cryst.* **24**, 946-950.
47. Merritt, E.A. & Murphy, M.E.P. (1994). Raster3D Version 2.0 – a program for photorealistic molecular graphics. *Acta Crystallogr. D* **50**, 869-873.
48. Barton, G.J. (1993). ALSCRIPT: a tool to format multiple sequence alignments. *Protein Eng.* **6**, 37-40.
49. Esnouf, R.M. (1997). An extensively modified version of MolScript that includes greatly enhances coloring capabilities. *J. Mol. Graph.* **15**, 132-134.

Because *Structure with Folding & Design* operates a 'Continuous Publication System' for Research Papers, this paper has been published on the internet before being printed (accessed from http://biomednet.com/cbiology/str). For further information, see the explanation on the contents page.